Supplementary Information

Freeze Casting of Porous Monolithic Composites for Hydrogen Storage

George M. Neville, Rajan Jagpal, Joseph Paul-Taylor, Mi Tian, Andrew D. Burrows, Christopher R. Bowen, Timothy J. Mays

S.1 Polymer Characterisation

The successful synthesis of PIM-1 was inferred from chemical characterisation techniques. ^{1}H NMR spectra (Figure S1) were recorded using an *Agilent* 500 MHz NMR spectrometer at room temperature, where PIM-1 samples were dissolved in deuterated chloroform ($CDCl_3$) at relatively high concentrations (40 mg ml^{-1}) to ensure good quality spectra. All spectra were processed in *Mestrelab MNova 11.0* software, where spectra were baseline corrected and line broadening systematically used to ease analysis.

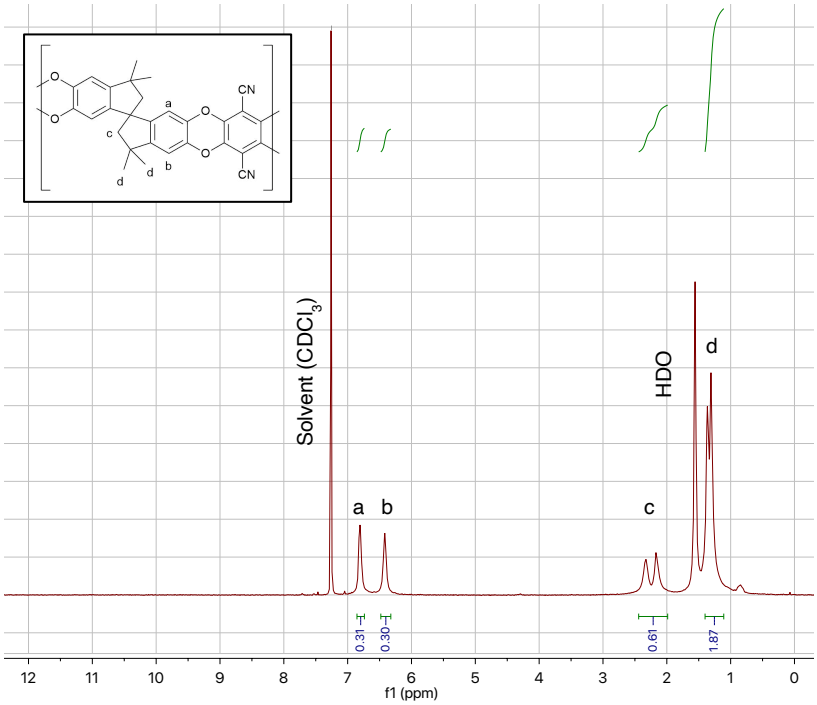

Figure S1. ^{1}H NMR spectrum PIM-1 [$CDCl_3$]: δ 6.80 (2H, s, H_a), 6.40 (2H, s, H_b), 2.00-2.50 (4H, d, H_c), 1.29-1.37 (12H, d, H_d).

Terephthalonitrile (TTN) moieties could not be identified using this technique due to the lack of proton environments, and consequently neither could any unreacted monomer of this species. Although gel permeation chromatography (GPC) was predominantly used to monitor the loss of residual low molecular weight polymer post-purification, chromatograms were also used as a means of identifying impurities (Figure S2). PIM-1 solutions in THF (2 mg ml^{-1}) were submitted to an *Agilent GPC 1260 Infinity* system, using two PLgel 5 μm MIXED-D 30 cm x 7.5 mm columns with a guard column PLgel 5 μm MIXED Guard 50 x 7.5 mm. The column oven was maintained at 35 °C, with GPC-grade THF as the eluent at a flow rate of 1.00 ml min^{-1} and refractive index detection. Whilst the system was calibrated against 12 narrow molecular weight polystyrene standards with a range of M_w from 1050 Da to 2650 kDa, somewhat similar to PIM-1, it is likely unaccounted for interactions between the solute and stationary phase will cause disparity between measured weights and absolute values. All GPC chromatograms were subsequently analysed using *Agilent GPC/SEC* software to extract M_n and PDI values (Table S1).

From the chromatogram, a bimodal size distribution is evident. *Peak 1* almost certainly represents high molecular weight polymer. Polymer weights (M_w) were found to be 111 kDa, constituting approximately 240 units of each monomer. Despite extensive purification, *Peak 2* likely represents partially or unreacted monomer, however, this did not appear to effect the efficacy of film formation and so was deemed acceptable for use.

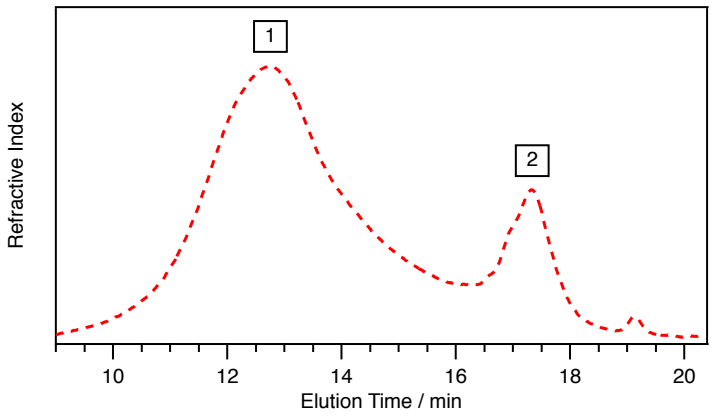

Figure S2. GPC chromatogram for PIM-1 powder with labelled peaks (boxes).

Table S1. Physical properties extracted from chromatogram for PIM-1.

Peak	M_w / kDa	M_n / kDa	PDI
1	111.4	26.8	4.2
2	1.5	1.2	1.2

S.2 SEM Comparison of Powders

Figures S3a-c show the PIM-1 powder at various magnifications, and Figure Sd-f the AX21 powder. Whereas PIM-1 has a characteristic cauliflower-like or fluffy appearance, AX21 is visibly more platelet-like, with a greater occurrence of flat facets than PIM-1. This is translated when cast into films and can be used to distinguish the materials to assess homogenous mixing.

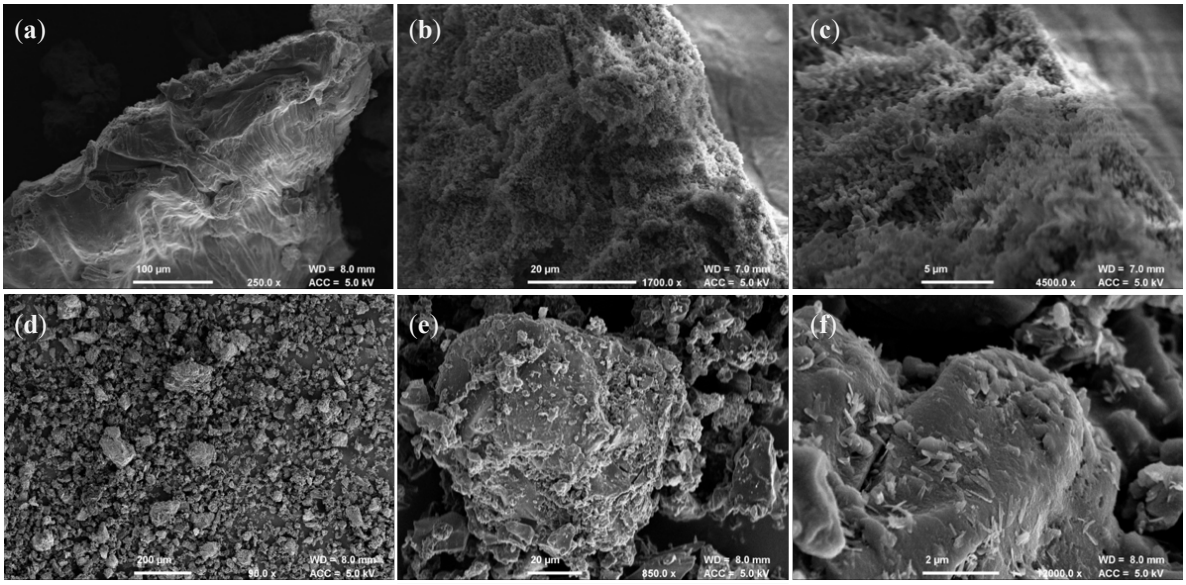

Figure S3. SEM micrographs of a (**a-c**) PIM-1 and (**d-f**) AX21 powder sample at various magnifications.

S.3 DMTA of PIM-1 Film

PIM-1 films were submitted to tensile testing by dynamic mechanical thermal analysis (DMTA) to corroborate the expected mechanical properties of PIM-1, as well as to demonstrate the inherent barriers to thermo-forming techniques. A scalpel was used to cut films into thin strips (5 by 40 mm) before being clamped between two single cantilever clamps in a *Mettler Toledo DMA1 Star* system. These were then sealed in a temperature-controlled container, equipped with a rapid heating element capable of ramping rates of 3 K min^{-1}. A liquid nitrogen canister allowed for an accessible temperature range between approximately -170 – 400 °C. The clamps were then programed to oscillate at an amplitude of 20 µm (0.005 strain) at a frequency of 1 Hz, monitoring the Young's modulus of the film against temperature.

It can be seen in Figure S4a that as temperature was increased, the stiffness of the material gradually decreased due to the loss of intermolecular interaction between polymer chains. At room temperature, a Young's modulus of approximately 700 MPa was achieved, in agreement with the average 1 GPa reported in literature [1]. Although stiffness should theoretically remain constant irrespective of forming method, discrepancies between testing standards and also the quality of synthesis may explain this divergence.

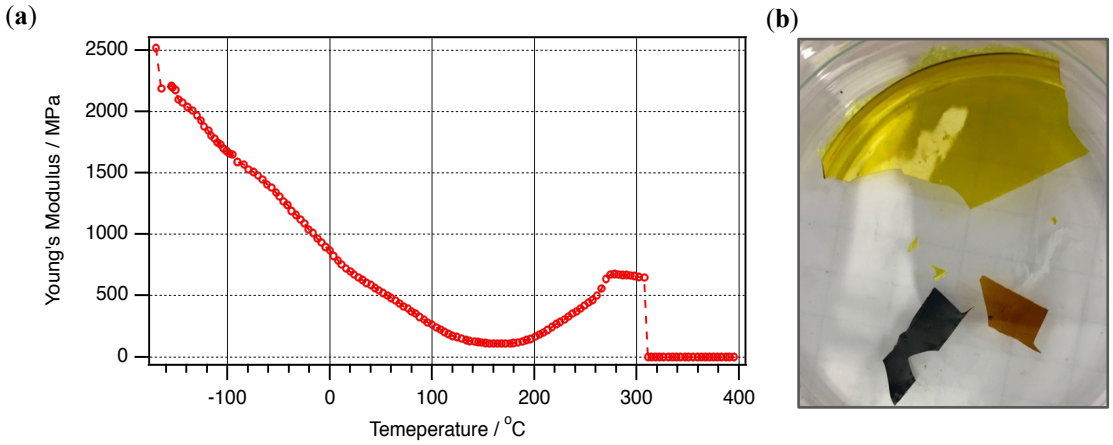

Figure S4. (**a**) DMTA results for PIM-1 film. (**b**) Colour transition from yellow to brown upon heating.

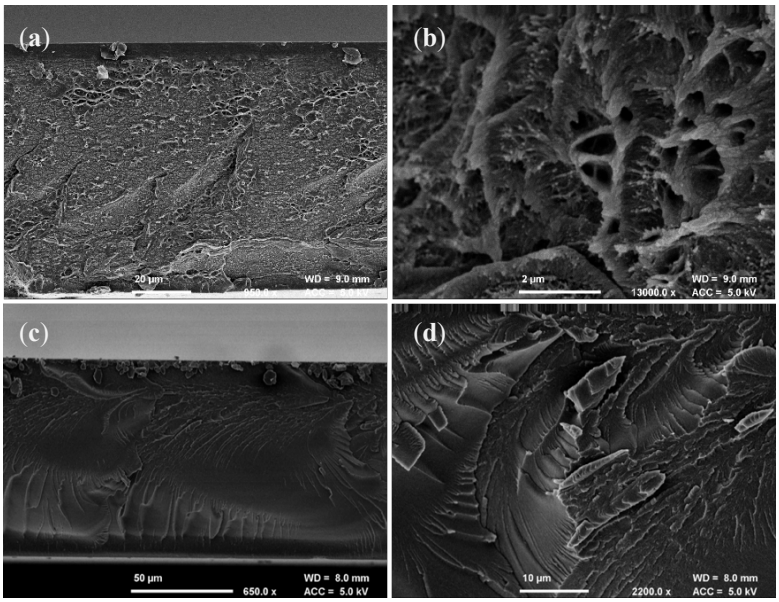

Figure S5. SEM micrographs of PIM-1 film cross sections (**a-b**) before and (**d-f**) after self-crosslinking.

Interestingly, above 150 °C, stiffness increased until eventual failure at 310 °C. Previously, it was identified in literature that between 250 – 400 °C self cross-linking can occur [2], resulting in increased brittleness and a change of colour to dark brown or black (as demonstrated in Figure S4). Pore widths were also reduced. SEM of the PIM-1 film here, both pre (Figure S5a-b) and post (Figure S5c-d) heat treatment, revealed a transition to a smoother and comparatively featureless cross-section expected to perturb gas transport.

S.4 Foams

To produce foams as described in the main article, a more traditional anisotropic freeze casting technique was used. Here, a relatively thin, open-ended silicone mould was stuck to a conductive aluminium base, before being filled with precursor chloroform solutions (100 mg ml^{-1}) for freezing. Once under vacuum however, solutions rapidly began to boil given the volatility of the solvent used (Figure S6a-b), producing mechanically weak, void-filled structures (Figure S6c-d). Hence various adaptations were made to the process to try preserve chloroform in a frozen state (summarised in Figure S7a-b).

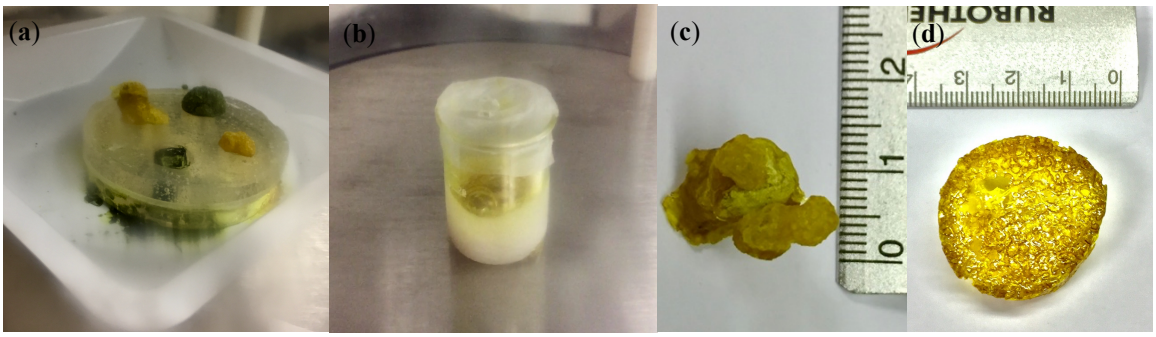

Figure S6. (**a-b**) Boiling of frozen precursor chloroform solutions upon application of vacuum regardless of mould volume and (**c-d**) resulting PIM-1 foams.

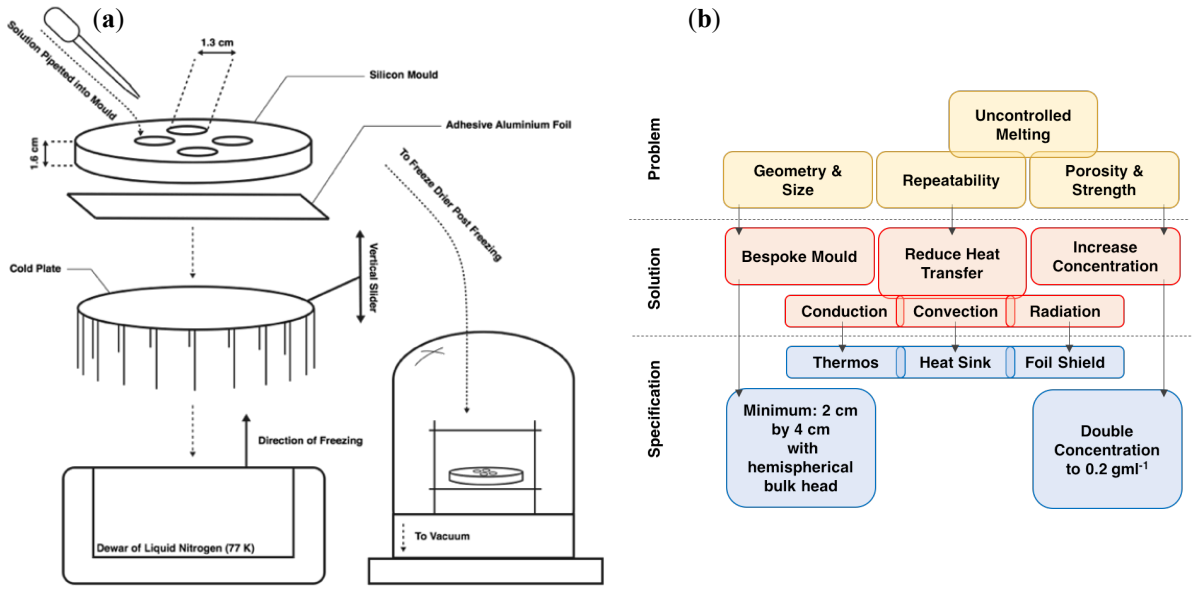

Figure S7. (**a**) Schematic summary of the anisotropic freeze casting method used to produce foams. (**b**) problem-solution matrix for reasoning behind adaptions made to this process to preserve frozen chloroform to improve repeatability and strength as well as other project goals such as geometry control.

S.5 Additive Manufacture of Elastomer Mould

Figure S8 outlines the SLA *FormLabs* equipment used for additive manufacture of the elastomer mould used within the main article, including the *Form2* printer, the *FormWash* and the *FormCure*.

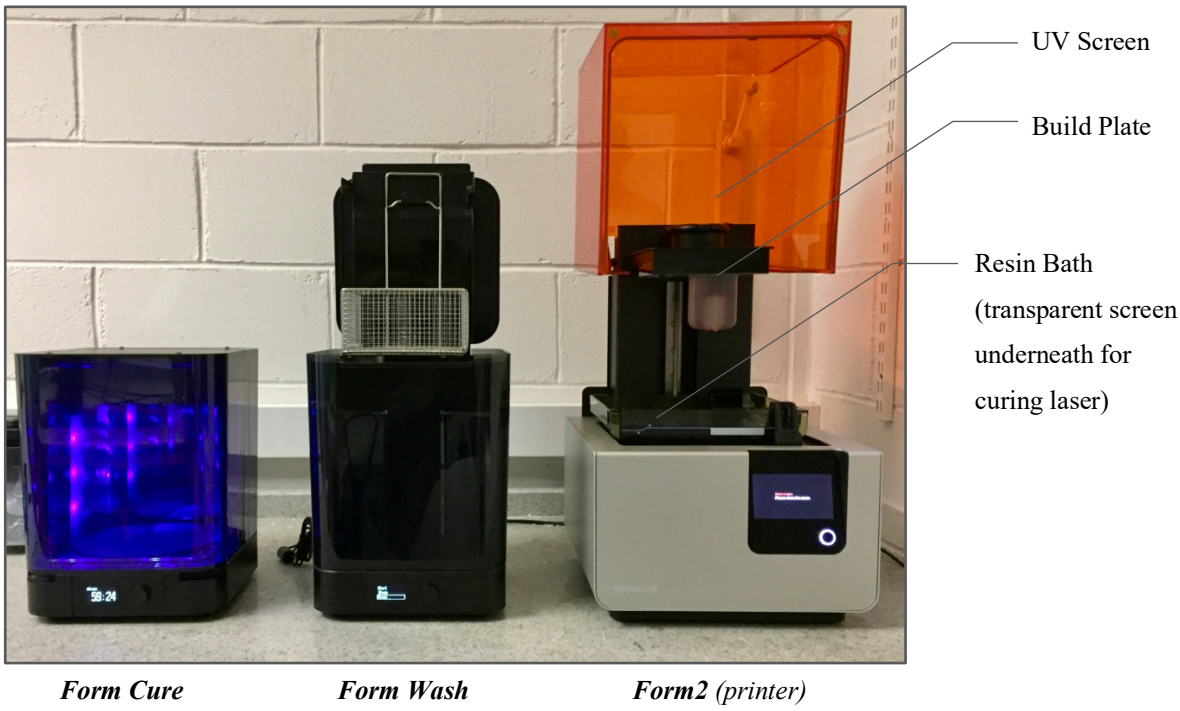

Figure S8. Equipment used to SLA print the elastomer mould, including the *Form 2* printer, *Form Wash* & *Form Cure*.

Once printed, parts need to be washed and cured to remove excess resin (Figure S9a). However, even after curing, it was noticed that the inside of the mould cavity remained somewhat tacky with uncured resin. This was likely because it was difficult for UV to penetrate this particular location. To resolve this, the cavity was first filled with water to exclude oxygen, before being placing outside in bright sunshine for 2-3 hours, resulting in the finished mould (Figure S9b-c).

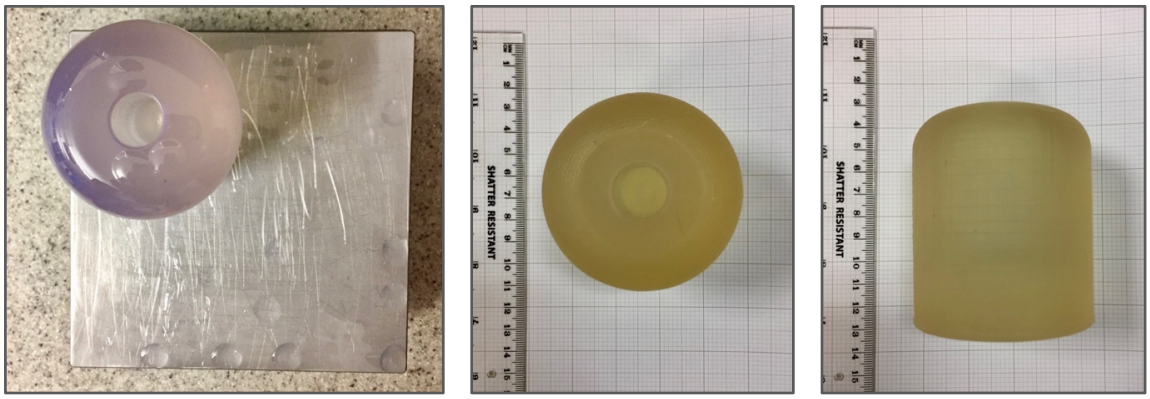

(**a**) (**b**) (**c**)

Figure S9. (**a**) SLA-printed mould immediately after print and (**b-c**) final mould post processing.

S.6 Convection during Freezing

As discussed in the main text, it is believed that the internal structures found within monoliths arise from a coupling between convection and the hemispherical geometry of the mould cavity. To aid understanding, a simple schematic of how voids would be excluded during freezing is illustrated in Figure S10. Here, black arrows indicate cold transfer from liquid nitrogen to the cavity, and how this varies between radial and linear areas of the mould. Red and blue arrows indicate where warmer chloroform would rise and exclude a central void and where cooler, denser chloroform would descend, respectively. At the hemispherical end, this creates an hourglass structure, and above this, planar voids where the cavity instead has parallel sides. Further along this axis of the monolith, less and less thermal protection was provided by the mould, and hence precursor solutions become more likely to evaporate, rather than sublime, nearer this open terminus, sometimes inducing bubbling or ballooned structures.

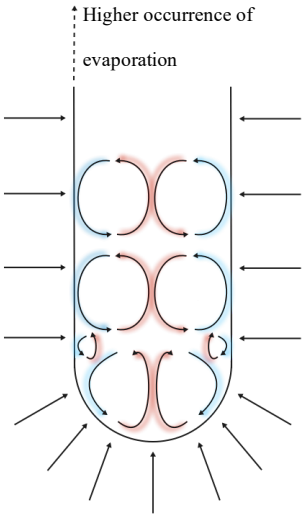

Figure S10. Schematic of convection inside mould cavity during freezing. Black arrows indicate cold transfer to the cavity. Red and blue arrows the movement of warmer and cooler solution respectively.

References

[1] Polak-Kraśna, K.; Dawson, R.; Holyfield, L.T.; Bowen, C.R.; Burrows, A.D.; Mays, T.J. Mechanical characterisation of polymer of intrinsic microporosity PIM-1 for hydrogen storage applications. *Journal of Materials Science* **2017**, *52*, 3862-3875, doi:10.1007/s10853-016-0647-4.

[2] Li, F.Y.; Xiao, Y.; Chung, T.-S.; Kawi, S. High-Performance Thermally Self-Cross-Linked Polymer of Intrinsic Microporosity (PIM-1) Membranes for Energy Development. *Macromolecules* **2012**, *45*, 1427-1437, doi:10.1021/ma202667y.